ASTROBIOLOGY
Volume 11, Number 6, 2011

DOI: 10.1089/ast.2011.0605

Genesis and Preservation of a Uranium-Rich Paleozoic Epithermal System with a Surface Expression (Northern Flinders Ranges, South Australia): Radiogenic Heat Driving Regional Hydrothermal Circulation over Geological Timescales

Joël Brugger,[1,2] Pierre-Alain Wülser,[1,2] and John Foden[1]

Abstract

The surface expressions of hydrothermal systems are prime targets for astrobiological exploration, and fossil systems on Earth provide an analogue to guide this endeavor. The Paleozoic Mt. Gee–Mt. Painter system (MGPS) in the Northern Flinders Ranges of South Australia is exceptionally well preserved and displays both a subsurface quartz sinter (boiling horizon) and remnants of aerial sinter pools that lie in near-original position. The energy source for the MGPS is not related to volcanism but to radiogenic heat produced by U-Th-K-rich host rocks. This radiogenic heat source drove hydrothermal circulation over a long period of time (hundreds of millions of years, from Permian to present), with peaks in hydrothermal activity during periods of uplift and high water supply. This process is reflected by ongoing hot spring activity along a nearby fault. The exceptional preservation of the MGPS resulted from the lack of proximal volcanism, coupled with tectonics driven by an oscillating far-field stress that resulted in episodic basement uplift. Hydrothermal activity caused the remobilization of U and rare earth elements (REE) in host rocks into (sub)economic concentrations. Radiogenic-heat-driven systems are attractive analogues for environments that can sustain life over geological times; the MGPS preserves evidence of episodic fluid flow for the past ~300 million years. During periods of reduced hydrothermal activity (*e.g.*, limited water supply, quiet tectonics), radiolytic H_2 production has the potential to support an ecosystem indefinitely. Remote exploration for deposits similar to those at the MGPS systems can be achieved by combining hyperspectral and gamma-ray spectroscopy. Key Words: Epithermal system—Sinter deposit—Preservation—Zircon geochronology—Uranium and REE mobility—Radiogenic heat—Exploration targeting. Astrobiology 11, 499–508.

1. Introduction: Fossil Epithermal Systems

The surface expression of terrestrial volcanogenic epithermal systems—including geysers and hydrothermal pools—is among the most spectacular signs of ongoing geological activity on Earth (*e.g.*, Yellowstone National Park, New Zealand, Kamchatka Peninsula; Pirajno and Van Kranendonk, 2005). These systems provide direct insight into ore-forming processes. Most importantly, they support diverse ecosystems and may have played a direct role in the development of life on Earth (Pace, 2001), given that they provide sources of water, heat, and chemical energy (*e.g.*, molecular hydrogen, sulfur, reduced carbon) conducive to sustaining life. Hence, surface expressions of hydrothermal systems are a prime target for exploration for life in the Solar System (Thomas and Walter, 2002; Schulze-Makuch *et al.*, 2007; Shapiro and Schulze-Makuch, 2009). Evidence of silica-rich hydrothermal deposits linked to martian volcanic activity has been reported recently (Squyres *et al.*, 2008; Skok *et al.*, 2010).

Preservation of the surface expression of aerial epithermal systems in Earth's fossil record is poor and, in fact, as rare as the preservation of morphological volcanoes due to the dynamic environment in which they usually form. The oldest such systems described to date are linked to proximal volcanism and are Devonian in age [Drummond Basin, Australia, Walter *et al.* (1998); and Rhynie cherts, Scotland,

[1]Tectonics, Resources and Exploration, School of Earth and Environmental Sciences, The University of Adelaide, Adelaide, Australia.
[2]Division of Mineralogy, South Australian Museum, Adelaide, Australia.

Preston and Genge, (2010)]. This contrasts with seafloor hydrothermal systems, pristine examples of which are known to date as far back as the Early Archean and contain the earliest unequivocal fossils (Pirajno and Van Kranendonk, 2005).

In this paper, we use geological, textural, geochemical, and geochronological evidence to document an exceptionally well-preserved Palaeozoic epithermal system with a surface expression, the Mt. Gee–Mt. Painter system (MGPS) in the Northern Flinders Ranges, South Australia. We demonstrate that the preservation of this system, its unusual chemistry characterized by high levels of uranium and rare earth element (REE) enrichment, and the long-standing episodic hydrothermal activity (>120 Ma; Devonian to Permian, with low-level activity continuing to this day) around Mt. Gee are due to the unusual tectonic environment in which the system developed and the geochemistry of the host rocks. We also show that the MGPS represents an amagmatic epithermal system driven by proximal radiogenic heat. We argue that analogous systems are prime targets for exploration for life in the Solar System.

The Mt. Gee–Mt. Painter areas are of exceptional value in that they are the oldest well-preserved, continental epithermal systems with a surface expression. The history of this region includes the early recovery of radium in 1910–1914 (Brugger *et al.,* 2003) and periods of intense mineral explorations during uranium "booms" (1960s and present). The outcrops, rocks, and minerals are spectacular, and the potential association of the system with radiogenic heat related to the regional abundance of radioactive minerals in the basement rocks of the Northern Flinders Ranges makes this setting unique among Paleozoic continental epithermal systems.

2. Analytical Methods

2.1. Zircon typology and morphology

Heavy minerals were extracted and concentrated from crushed rocks by panning and micro-jigging; then they were further separated by permanent magnets. To avoid cross contamination due to the use of heavy liquids and electromagnets, the whole procedure was performed by hand. Final concentrates were examined under a binocular microscope and hand picked. Since one of the aims of the zircon study was to provide an upper age for the mineralization that crosscuts these sediments, it was important to discover the youngest zircons in the population. Such "young" zircons are likely to be rare, and random sampling may not be an adequate strategy. Here, we sorted zircons according to typology (Pupin, 1980) to increase the probability of identifying a small population of young zircons. A combination of dating and typology was used, for example, by Willner *et al.* (2003) to improve the determination of sedimentary provenances, and this method is particularly well suited for the Mt. Gee samples that are dominated by Mesoproterozoic zircons with distinctive typology. The sorted zircons were mounted in epoxy resin and polished for laser ablation–inductively coupled plasma mass spectrometer (LA-ICPMS) analysis.

2.2. LA-ICPMS geochronology and trace elements analyses

Laser ablation–inductively coupled plasma mass spectrometer measurements were conducted at Adelaide Microscopy. The detailed technique and procedure used for zircon analysis were described by Reid *et al.* (2006), and only a summary of the acquisition parameters is provided here. Ablation was performed with a 213 nm Nd-YAG laser (pits 40 μm in diameter). The ablated material was carried by an Ar-He gas medium to an Agilent 7500 quadrupole inductively coupled plasma mass spectrometer. The data were corrected for instrument drift and the isotopic ratios calculated with the GLITTER software (van Achterbergh *et al.,* 1999). For geochronology, the following isotopes were measured: ^{204}Pb, ^{206}Pb, ^{207}Pb, ^{208}Pb, ^{232}Th, ^{238}U. The standard used for calibration is a gem-quality red zircon, GJ: ^{207}Pb/^{206}Pb age is 608.5 ± 0.4 Ma, ^{206}Pb/^{238}U is 600.7 Ma, and ^{207}Pb/^{235}U is 602.2 Ma (Jackson *et al.,* 2004) with undetectable ^{204}Pb with current LA-ICPMS settings. Common lead correction was applied by using the global second-stage Pb reservoir model of Stacey and Kramers (1975). Trace elements were analyzed by using a NIST612 glass standard, with Zr as an internal standard (stoichiometric value corrected for the Hf contents).

3. Geology and Tectonic Setting of the MGPS

The MGPS is located in the $60 \times 10\,km^2$ Mt. Painter Inlier (MPI) of mainly Mesoproterozoic rocks that outcrop as a window in the Neoproterozoic to Cambrian rocks of the northern end of the Adelaide Geosyncline (Coats and Blissett, 1971; Teale and Flint, 1993). The inlier is bound on its eastern margin by the Paralana Fault. This long-lived structure is still active as a reverse fault and has been the locus of the recent uplift that has exposed the Mt. Painter basement since the Late Miocene. The MPI consists of voluminous Mesoproterozoic granitic and felsic volcanic rocks (1576–1551 Ma) that intrude metamorphosed Mesoproterozoic volcano-sedimentary sequences (Radium Creek Metamorphics; Fanning *et al.,* 2003). The Cambro-Ordovician Delamerian metamorphism (514–485 Ma; Foden *et al.,* 2006) reached amphibolite facies in the MPI but was limited to low grade in the central Adelaide Geosyncline. The sharp temperature gradient toward the MPI has been explained as a consequence of contact metamorphism with the MPI basement heated by the radiogenic heat from the Mesoproterozoic granites, some of which are extremely enriched in U and Th (Neumann *et al.,* 2000). The British Empire granite located in the central part of the inlier, originally thought to be Delamerian (~500 Ma), has recently been dated at 441 ± 2 Ma (Elburg *et al.,* 2003).

Thermochronology (K-Ar and Ar-Ar, McLaren *et al.,* 2002; apatite fission tracks, Mitchell *et al.,* 2002) revealed a multistage post-Delamerian cooling and uplift history. Cooling stages at ~430 and 400 Ma were followed by a major cooling stage at 330–320 Ma that brought the MPI below 200°C. Slow cooling from >110°C occurred during the Late Carboniferous–Early Permian, and a final cooling episode took place during the Paleocene to the Eocene. Foster *et al.* (1994), found evidence for the flow of large volumes of fluids during the Middle Tertiary in the Paralana Fault. Small-scale hydrothermal activity still persists in the area, as shown by the Paralana Hot Spring that emerges at a temperature of ~65°C (Brugger *et al.,* 2005, 2011).

4. Architecture of the Mt. Gee–Mt. Painter System

We summarize here observations that show that the MGPS preserves the surface expression of an epithermal

system (pools and sinters of the "Mt. Painter Unit"), as well as a shallow subsurface boiling horizon ("Mt. Gee Unit").

The MGPS occurs as a semi-stratiform complex that unconformably overlies and partly intrudes heavily metasomatized (feldspatization and chloritization) Radium Creek Metamorphics. The Mt. Gee and Mt. Painter Units are subhorizontal (Fig. 1); together these units correspond to the "Mt. Gee Sinter" of Drexel and Major (1987). The Mt. Gee Unit is a massive, vuggy quartz unit with east-plunging roots. Abundant geopetal features indicate near-surface deposition with little reorientation and include stalagmites of jasper and quartz in cavities (Fig. 2d); hematitic, silica-rich hydrothermal sediments filling cavities (Fig. 2f); and rhythmic textures that are commonly asymmetric relative to depth (*e.g.,* Fig. 2e). A large part of the quartz was deposited as chalcedony, as indicated by the abundance of "flamboyant" or "plumose" quartz (Dong *et al.,* 1995). This early chalcedony is commonly overgrown by equant, anhedral grains of milky quartz. Fournier (1985) interpreted such textures as indicating crystallization from gelatinous amorphous silica from highly supersaturated solutions (*i.e.,* fast cooling or boiling). Quartz that grows freely in open cavities often overgrows an acicular mineral (Fig. 2c), which shows lozenge sections and common arrowhead twinning. The original mineral, laumontite, is always completely dissolved in the massive Mt. Gee Unit but is preserved locally in the roots of the system. Other evidence for mineral dissolution or pseudomorphosis includes abundant cubes and octahedrons of fluorite (Fig. 2e), platy crystals of barite, and rare ditrigonal prisms probably of tourmaline. The root of the Mt. Gee Unit contains numerous quartz veins inside feldspathized metasediments of the Radium Creek Metamorphics. Locally, these veins contain preserved fluorite, laumontite, and barite. Hematite-rich lenses within the Mt. Gee Unit display a range of textures (Fig. 1), from massive coarse-grained to "leopard" (0.5–3 cm diameter spherical coarse hematite-rich aggregates in quartz, often displaying rhythmic distribution of the size and density of the aggregates) to rhythmic (Fig. 2e). These textures all point out to a near-surface, dynamic hydrothermal environment and are consistent with boiling underneath a surface epithermal system. Fluid inclusion studies are also consistent with intermittent boiling of fairly pure water at 100–140°C and 1–5 MPa during the epithermal stage (Bakker and Elburg, 2006). The geochemistry of the MGPS is unusual in that the hematite-rich parts [Fe/(Fe + Si) >0.3] are enriched in light REE, Mo, Nb, and U (Fig. 3). Recent exploration delineated total resources of >30 kton U_3O_8 and >50 kton rare earth oxide (www.marathonresources.com.au). Microscopic studies revealed the presence of molybdenite, Th-poor monazite-(Ce), pitchblende, and a rare, collomorph, hydrated U-Y-phosphate (Fig. 2g). The collomorph nature of the latter mineral and the fact that it overgrows epithermal pyrite indicate that U and REE were indeed mobile during the epithermal stage. However, the epithermal stage in the MGPS clearly overprints higher-temperature hydrothermal events, and the main period of U mobility remains poorly understood (see below).

The Mt. Painter Unit directly overlies the Mt. Gee Unit and is preserved only on the summit of Mt. Painter (Fig. 1). It consists mainly of fine-grained hematite-quartz rocks, with many relicts of subhorizontal layering. The unit is heavily silicified, and this silicification often obliterates the layering. Evidence of graded bedding is preserved locally (Fig. 2h). The Mt. Painter Unit commonly contains angular clasts (millimeters to 10 cm) of the Mt. Gee Unit that can also be distributed as layered deposits. In Fig. 2i, one layer contains relatively large, angular, internally layered clasts, while another contains sub-centimeter-sized quartz clasts. These clasts are interpreted to represent fragments of epithermal quartz ejected during explosive events, which landed within chemical sediments forming in surface hydrothermal pools ("hydrothermal eruption;" Hedenquist and Henley, 1985). The MGPS also contains enigmatic conglomerate sheets, referred to as "pebbles dikes" (Coats and Blissett, 1971). Typically, the pebbles dikes are matrix-supported diamictite conglomerates. The clasts are well rounded and consist mainly of quartzite and rhyolite. The pebbles dikes occur usually as disjointed bodies no more than a few meters in extent, but on the western side of Mt. Gee they grade into clast-supported conglomerates, which are clearly of fluvial origin (Fig. 2b).

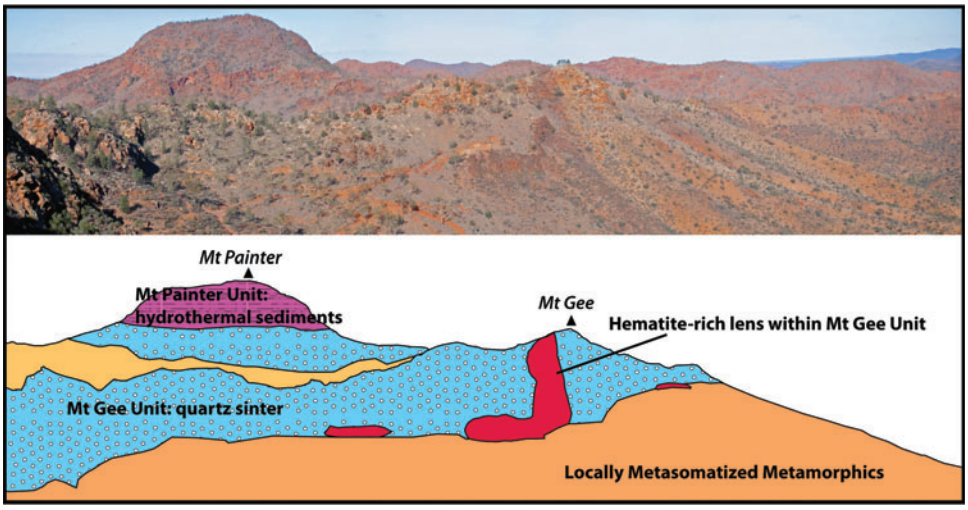

FIG. 1. Geomorphology of the Mt. Gee–Mt. Painter epithermal system. View toward the southeast. Color images available online at www.liebertonline.com/ast

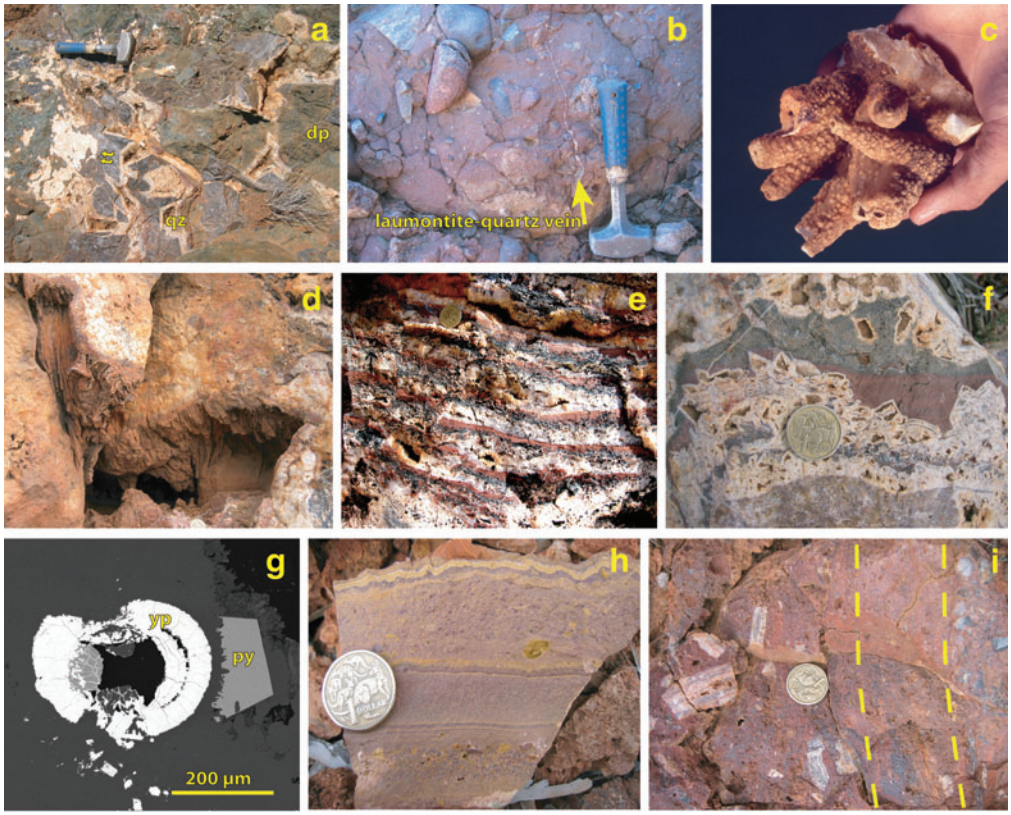

FIG. 2. Textures in the MGPS, up stratigraphy from below Mt. Gee Unit (**a**), to Mt. Gee Unit (**b**–**g**), to Mt. Painter Unit (**h**, **i**). (a) Magmatic hydrothermal titanite (tt) - diopsite (dp) vein overprinted by epithermal quartz (qz) veins. Southeast of Mt. Gee. (b) Fluvio-glacial conglomerates (pebbles dike), crosscut by a quartz-laumontite veinlet. Mt. Gee West. (c) Typical epithermal quartz growing in cavities around acicular crystals of laumontite (now dissolved), Radium Ridge. (d) Vuggy quartz, with stalactites of ferroan quartz in original orientation, Mt. Gee. (e) Asymmetric rhythmic quartz veining, with coarse hematite (black) at the bottom and red quartz with fine-grained hematite (red) at the top. Pure crystalline quartz grew around a central cavity, Mt. Gee. (f) Cavity filled with hydrothermal sediments; a change in color due to a change in the oxidation state of Fe records the paleo-orientation. Also note pseudomorphosis of former fluorite crystals by quartz, Mt. Gee. (g) Collomorph U-Y-phosphate mineral, Core GE9903, 319 m. Scale bar = 200 μm; py, pyrite; yp, Y-U-phosphate. (h) Compositional and granulometric layering in the Mt. Painter Unit, interpreted as representing sedimentation in a sinter pool. (i) Elements of quartz sinter inside fine-grained hematite-quartz "sediment," interpreted as resulting from hydrothermal eruptions. Dashed lines emphasize the layering, marked by different types of clasts. Color images available online at www.liebertonline.com/ast

Stratigraphically below the Mt. Gee Unit, hematite ± magnetite breccia bodies mineralized in U and Mo (uraninite, molybdenite) were the focus of U exploration in the 1940s and 1960s (Coats and Blissett, 1971), and currently by Marathon Resources. Based on the similarities in mineralogy and geochemistry and spatial association, these breccia bodies were interpreted to represent a deeper expression of the hydrothermal system that underpinned the Mt. Gee–Mt. Painter system. Two occurrences of high-temperature hydrothermal mineralization overprinted by the epithermal stage suggest a continuum from magmatic hydrothermal to epithermal (Bakker and Elburg, 2006; Elburg *et al.,* 2003). Pegmatitic titanite-diopside-fluorapatite veins southeast of Mt. Gee formed at 510 ± 20°C, 130 ± 10 MPa (Fig. 2a; Bakker and Elburg, 2006). At the base of the Mt. Gee unit, the Number 2 Workings expose a lens of massive coarse-grained hematite with a fine-grained monazite-(Ce), xenotime-(Y), and Ca-Fe-phosphate matrix and locally abundant ishikawaite-Fe-rich euxenite (Brugger *et al.,* 2004, 2011).

5. Geochronology

In this section, we show that the MGPS is late Paleozoic in age, the pebbles dikes represent most probably Permian fluvio-glacial sediments, and the MGPS overprints an earlier magmatic hydrothermal mineralization.

The age of the MGPS remains controversial. Elburg *et al.* (2003) proposed a Late Ordovician age based on new geochronological results and in particular a correlation between the age of the British Empire granite (441 ± 2 Ma) and that of the titanite from the titanite-diopside veins (443 ± 3 Ma). Ca-rich monazite-(Ce) from the Mt. Gee Unit is rich in common Pb and led imprecise ages of 440 ± 50 Ma (Pidgeon, 1979; Elburg *et al.,* 2003). These radiochronology results contrast with the paleomagnetic data of Idnurm and Heinrich (1993), which suggest that two separate Permo-Carboniferous thermal events affected the metasomatic breccia on Radium Ridge, whereas only one such event was recorded in the Mt. Painter Unit (Fig. 4).

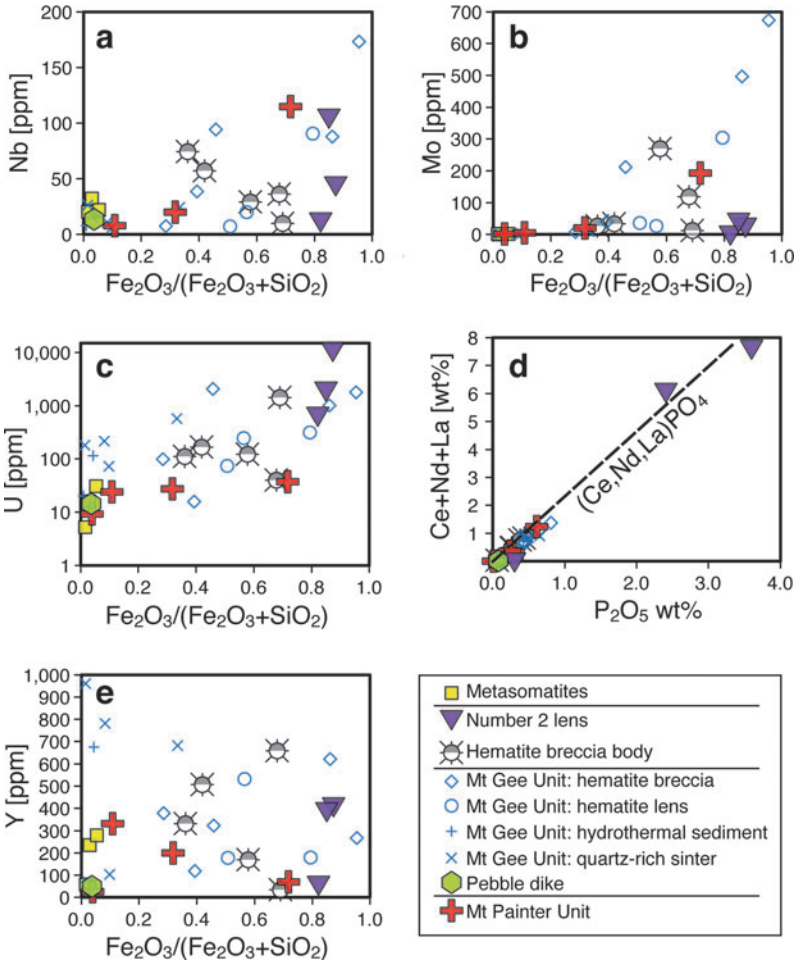

FIG. 3. Geochemistry of the Mt. Painter–Mt. Gee epithermal system. X-ray fluorescence data. The dashed line in (d) shows the mixing line for monazite, with a molar ratio of (Ce + Nd + La) : P = 1. Color images available online at www.liebertonline.com/ast

To further constrain the age of the epithermal activity, we extracted zircons from the matrix of three pebbles dike samples, including the conglomerate at Mt. Gee West and some matrix-supported facies on Mt. Gee East. The zircon populations are dominated by Mesoproterozoic zircons, which is consistent with a predominantly local origin of the matrix (Fig. 5). A minor population of Paleozoic (and Late Proterozoic) zircons, however, provides an insight into the source and origin of the pebbles dikes. The age of the youngest zircon is 315 ± 9 Ma; as the conglomerates are crosscut by

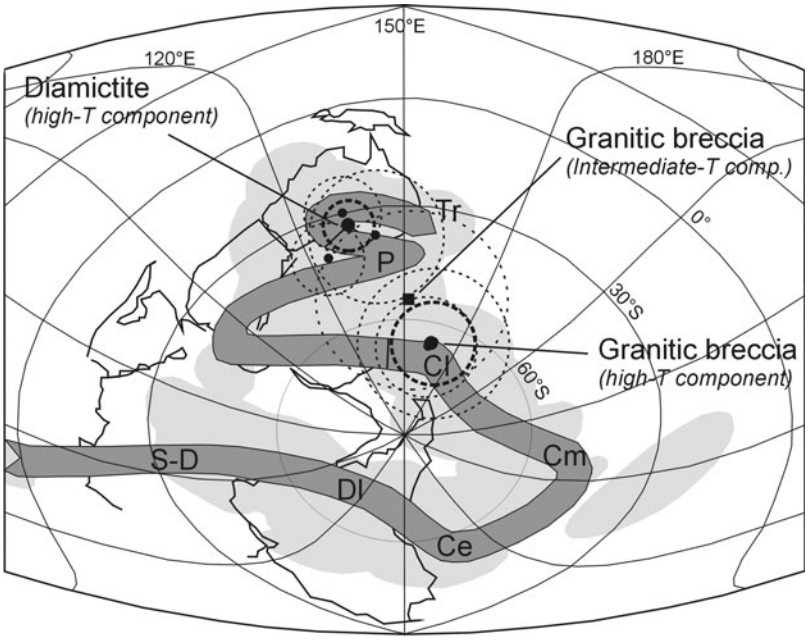

FIG. 4. Paleomagnetic data on Mt. Gee diamictite and granitic breccia (Idnurm and Heinrich, 1993), plotted relative to Australian paleomagnetic "model B" of Klootwijk (2010). S-D, Silurian-Devonian; Dl, Late Devonian; Ce, Early Cretaceous; Cm, Middle Carboniferous; Cl, Late Carboniferous; P, Permian; Tr, Triassic.

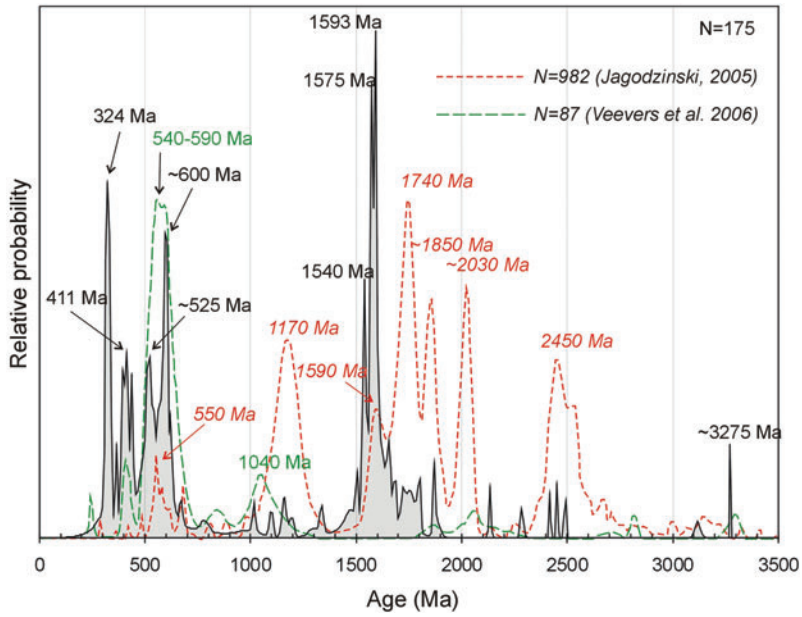

FIG. 5. Histogram showing the age distribution of zircons extracted from the matrix of the pebbles dike, compared with those of the Gawler Craton (Jagodzinski, 2005; Veevers *et al.*, 2006). Color images available online at www.liebertonline.com/ast

the latest stage of the epithermal mineralization (Fig. 2b), this zircon gives a maximum age for the youngest epithermal activity. The matrix contains a sizable population of 520–650 Ma zircons, which strongly suggests an Antarctic origin and transport via glaciers during the Late Carboniferous–Permian glaciation (Veevers *et al.*, 2006). This Antarctic origin is further confirmed by the occurrence of one zircon (age 637 ± 21 Ma) with an unambiguous alkaline (carbonatitic or kimberlitic) signature (Lu 1.76–4.06 ppm; Ta 0.36–0.93 ppm; Hf 1.06–1.31 wt %; $n = 5$; Belousova *et al.*, 2002).

We also analyzed davidite-(La) collected by Broughton (1925) and preserved at the South Australian Museum (G23810). Davidite, $(REE)(Y,U)(Ti,Fe)_{20}(O,OH)_{38}$, is a member of the crichtonite group and has the capacity to accommodate both U and Pb (Wülser *et al.*, 2005). The morphology and composition of the analyzed sample is consistent with a pegmatitic origin, its locality corresponding to the roots of the Mt. Gee system (coordinates 339675/6654725). The U-Pb isotopic data show a reverse discordance (Fig. 6a), with a $^{207}Pb/^{206}Pb$ age of 286 ± 6 Ma assuming a uranium loss at $t = 0$. The $^{204}Pb/^{206}Pb$ ratio is low and implies that the lead composition does not contain more than 1.2% common lead. Even with this correction, the $^{207}Pb/^{206}Pb$ apparent age remains close to ~290 Ma. Davidite also contains Th, and the ^{232}Th-^{208}Pb-^{204}Pb system gives a Delamerian 492 ± 20 Ma isochron age (Fig. 6b). These U-Th-Pb data suggest a Delamerian age for the formation of davidite within pegmatites, with a subsequent major uranium loss at 286 ± 6 Ma that did not affect the Th or Pb in the mineral. The new geochronology data (youngest zircon in pebbles dike at 315 ± 8 Ma; U leaching from davidite at 286 ± 6 Ma) hence support a Permian age (299–251 Ma) instead of a Devonian age for the epithermal system.

6. Preservation of a Late Paleozoic Amagmatic Epithermal System with Surface Expression

The keys to the formation, geochemistry, and preservation of the MGPS are the association with high-radiogenic-heat-producing rocks and a particular tectonic regime. Since the

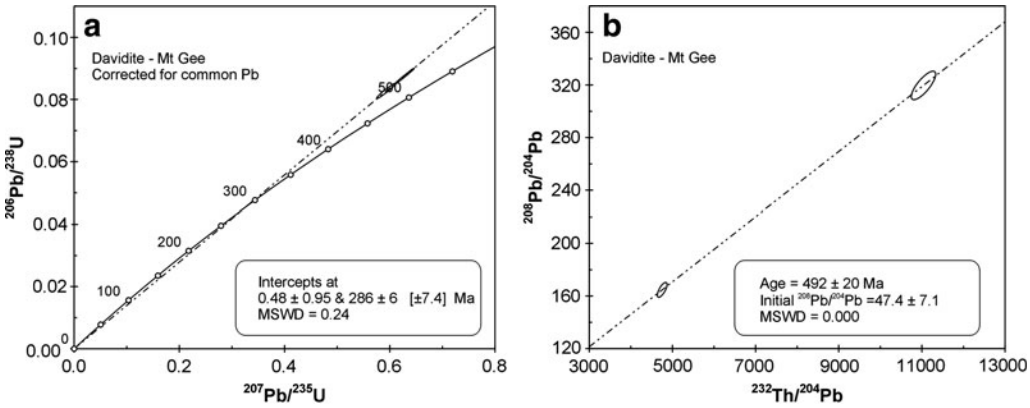

FIG. 6. Concordia diagrams for the davidite from Mt. Gee West. (**a**) Reverse discordant positions are interpreted to result from a U loss rather than a Pb loss, which is more stable in the davidite structure. (**b**) The composition of davidite also includes Th and common Pb; the 204-208-232 isochron indicates a mixing between a radiogenic inherited Pb, and a Delamerian ~490 Ma crystallization age; Th is thought to be immobile in davidite. Davidite was formed in a Delamerian pegmatite, which was subjected to a major hydrothermal event 286 ± 6 Ma ago. MSWD, mean square of weighted deviations.

start of the Palaeozoic, the MPI has been subjected to repeated episodes of uplift and erosion followed by burial. This oscillating history is probably correlated with far-field stress transfer from the Australian–Pacific plate margin (Sandiford and Quigley, 2009). The present-day mode is one of basement uplift and exhumation that leads to U release from the basement granites; part of this U was transported to roll-front type deposits in the adjacent Tertiary sedimentary basins to the east (the Beverley U deposit; Wülser *et al.*, 2011). This uplift is facilitated by reverse motion on the Paralana fault. The present tectonic mode contrasts with that in the late Mesozoic and early Tertiary when there was extensive marine transgression and the basement was not exposed (Wülser *et al.*, 2011).

The Permian age of the MGPS contrasts with the ~440 Ma magmatic hydrothermal activity recorded in the titanite-diopside veins and the hematite-REE-U-Nb mineralization at Number 2 workings, with >120 Ma between these events. The geochemical similarity between the magmatic hydrothermal mineralization and the MGPS epithermal deposits across such an extended time frame indicates that the ore geochemistry was strongly influenced by the chemistry of the U-Th-K- and REE-rich granites of the surrounding Mesoproterozoic basement and that hydrothermal events may have been repeated more than once.

In the absence of proximal volcanism, the establishment of the heat flow regime that drove hydrothermal circulation in the late Paleozoic most probably resulted from a combination of high geothermal gradients caused by the radiogenic basement (Neumann *et al.*, 2000) coupled with rapid uplift (McLaren *et al.*, 2002). Sandiford *et al.* (1998) estimated the mean heat production of the MPI to be 9.9×10^{-3} W m^{-3}, which is 4 times the heat production for average granites (2.5×10^{-3} W m^{-3}). This heat generation is due to high levels of U, Th, and K in the Mesoproterozoic granitoids. The MPI is currently uplifting, and low-level epithermal activity is indeed observed at the Paralana Hot Springs. The scale of the modern system is limited by low rainfall (Brugger *et al.*, 2005). An Early Permian age of the MGPS system means that epithermal activity took place during a glacial or interglacial interval. The sedimentology and zircon population (Fig. 7) of the pebbles dikes suggest that they are fluvio-glacial valley fill deposits preserved under and crosscut by the blanket of the epithermal MGPS. This is consistent with sharp topography at the time related to the rapid uplift. Interglacial meltdown may have provided the large amounts of water required for the formation of such a massive epithermal system, as well as contribution to uplift by isostasy.

There is no link between contemporaneous magmatism and the late Paleozoic MGPS epithermal system, and the MGPS appears to be the first documented continental Paleozoic amagmatic epithermal system. While modern continental epithermal systems of the scale observed at Mt. Gee/Mt. Painter are usually associated with volcanism, recent amagmatic epithermal systems occur in a number of settings. The closest analogues are hot springs located in and around the Idaho Batholith, where the energy that drives hydrothermal circulation is from the radioactive decay of K, Th, and U enriched in the batholith (van Middlesworth and Wood, 1998). Fehn *et al.* (1978) showed that the heat generated by such granites can account for the observed fluid flow, provided that enough porosity, for example in the form

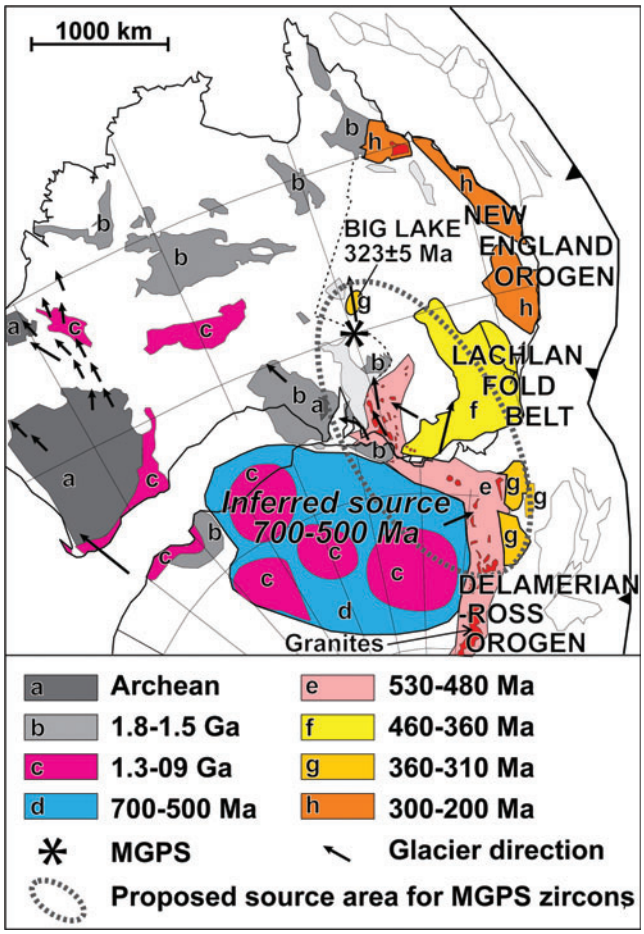

FIG. 7. Sources and ages of zircons as well as directions of transport during the Late Paleozoic glaciation. Modified after Veevers *et al.* (2006). Color images available online at www.liebertonline.com/ast

of fractures, is available. In the case of the Idaho Batholith, seismic activity is critical in maintaining the flow paths (Druschel and Rosenberg, 2001). On Earth, another important class of amagmatic epithermal systems are gravity-driven circulation cells in mountain ranges. In this case, radioactive heat sources have little influence, and gravity and fractures play the fundamental role in controlling the circulation of meteoric water to depths up to 5 km (Grasby and Hutcheon, 2001). The MGPS was not associated with orogenic activity.

7. Implications for Solar System Exploration

The MGPS illustrates that phenomenologically similar epithermal systems can be generated in very different settings, that is, proximal volcanogenic environments in modern Earth systems versus an amagmatic setting near a stable craton margin for the MGPS.

Magmatism, for the most part associated with plate tectonics and mantle convection, is the main driver for hydrothermal activity on Earth. On Mars, silica-rich deposits suggest the existence of shallow hydrothermal systems linked to volcanism (Skok *et al.*, 2010). Martian volcanism is not related to plate tectonics, and martian volcanic systems can be stable over hundreds of millions of years (*e.g.*, O'Neill

et al., 2007). Different mechanisms can drive hydrothermal systems in the absence of magmatism (Vance *et al.,* 2007). For example, serpentinization, a process in which high-temperature, anhydrous, highly reduced olivine and pyroxene-rich rocks react with water, liberates molecular hydrogen as well as thermal energy, driving low-temperature hydrothermal systems. A similar process is likely to have happened on Mars (Schulte *et al.,* 2006). Large meteorite impacts provide another locus for amagmatic hydrothermal activity (Naumov, 2002; Hode *et al.,* 2003; Lindgren *et al.,* 2009, 2010), and impact-related hydrothermal systems have been recently identified on Mars (Schulze-Makuch *et al.,* 2007; Schwenzer and Kring, 2009).

The MGPS is the first described example of an ancient (Paleozoic) continental surface hydrothermal system where the energy is provided by increased regional heat flow related to high U-Th-K contents of locally abundant (Mesoproterozoic) granitoids. Pulses of hydrothermal activity are related to vertical tectonics (rapid uplift), and the scale of the activity may be limited by water availability. The regional-scale enrichment in radioactive elements in the Mesoproterozoic rocks is the result of late magmatic and/or magmatic hydrothermal processes. Episodic large-scale hydrothermal activity occurred in the Mt. Painter area during the Paleozoic, and smaller-scale activity occurred throughout the Mesozoic and Cenozoic. To the present day, small-scale (limited by low rainfall) hydrothermal activity has occurred along the Paralana Fault (Foster *et al.,* 1994; McLaren *et al.,* 2002; Mitchell *et al.,* 2002; Brugger *et al.,* 2005).

Such radiogenic-heat-driven systems are attractive targets for biological exploration in the Solar System. On the one side, these systems are long lived (100–1000 million years), especially when compared to impact-related hydrothermal systems. Even in very large craters, such as in the ~1850 Ma Sudbury impact structure (Canada), hydrothermal activity was limited in time to around one million years (Ames *et al.,* 1998). These radiogenic-heat-driven systems can develop in the absence of volcanism or significant topography. Seismic activity, required to maintain a low-porosity fracture system, can be sustained for example by gravitational forces. Exploration for suitable targets can be made via remote sensing. The MGPS is associated with a characteristic alteration mineralogy that is recognizable, for example, via hyperspectral infrared spectroscopy (Thomas and Walter, 2002). Recently, the Kaguya Gamma-Ray Spectrometer produced a global lunar map of uranium distribution, which shows that uranium abundances reach up to 2 ppm, with an average of ~0.3 ppm (Yamashita *et al.,* 2010). This data set confirms that significant U fractionation took place on the Moon during the cooling of the magma ocean and subsequent volcanism (Shearer and Papike, 2005). More advanced fractionation is expected on planets with a longer magmatic history, while sedimentary U accumulations are likely on planets such as Mars.

The regional enrichments of U and REE necessary to sustain the MGPS can also play a critical role in supporting life. Uranium provides a radiolytic energy source as well as an oligomer catalyst for prototypical prebiotic homonuclear and dinuclear metalloenzymes (Adam, 2007). On Earth, production of H_2 by water radiolysis may fuel 10% of the metabolic respiration in oceanic sediments where organic-fueled respiration is lowest (Blair *et al.,* 2007); hence, radiolytic H_2 has the potential to support an ecosystem indefinitely (Lin *et al.,* 2006). Hydrothermal activity at Mt. Gee–Mt. Painter caused the remobilization of U to form deposits with grades up to several weight percent uranium. Such concentrations may evolve into sustained nuclear reactions early in the planet's history, which would contribute energetic and chemical conditions conducive to the appearance of life (Adam, 2007).

Given its Late Paleozoic age, the MGPS should contain both macro- and microfossils. Indeed, the modern expression of the hydrothermal system, the Paralana Hot Springs, contains abundant microbiota (Anitori *et al.,* 2002). However, neither macrofossils nor unambiguous microfossils have yet been reported from the MGPS (Carlton, 2002). We attribute this to the fact that most of the system has been eroded, with only a core preserved; this core is characterized by extensive, multiple silicification, which may be responsible for obliterating morphological evidence of fossils. A study of the organic content (for molecular biomarkers) in the MGPS would be of great interest for understanding the preservation of biosignatures in fossil epithermal systems.

Acknowledgments

We thank Jason Tilley and David Clark, who conducted their honours degree with topics related to the Mt. Gee system, for help in the field and for gathering preliminary data for this study. Graham Teale provided the key sample illustrated in Fig. 2g, and Stefan Ansermet provided the photograph shown in Fig. 2c. The article benefited from the insightful comments of two anonymous reviewers.

Disclosure Statement

No competing financial interests exist.

Abbreviations

LA-ICPMS, laser ablation–inductively coupled plasma mass spectrometer; MGPS, Mt. Gee–Mt. Painter system; MPI, Mt. Painter Inlier; REE, rare earth elements.

References

Adam, Z. (2007) Actinides and life's origins. *Astrobiology* 7:852–872.

Ames, D.E., Watkinson, D.H., and Parrish, R.R. (1998) Dating of a regional hydrothermal system induced by the 1850 Ma Sudbury impact event. *Geology* 26:447–450.

Anitori, R.P., Trott, C., Saul, D.J., Bergquist, P.L., and Walter, M.R. (2002) A culture-independent survey of the bacterial community in a radon hot spring. *Astrobiology* 2:255–270.

Bakker, R.J. and Elburg, M.A. (2006) A magmatic-hydrothermal transition in Arkaroola (northern Flinders Ranges, South Australia): from diopside–titanite pegmatites to hematite–quartz growth. *Contrib Mineral Petrol* 152:541–569.

Belousova, E.A., Griffin, W.L., O'Reilly, S.Y., and Fisher, N.I. (2002) Igneous zircon: trace element composition as an indicator of source rock type. *Contrib Mineral Petrol* 143:602–622.

Blair, C.C., D'Hondt, S., Spivack, A.J., and Kingsley, R.H. (2007) Radiolytic hydrogen and microbial respiration in subsurface sediments. *Astrobiology* 7:951–970.

Broughton, A.C. (1925) Radio-active ilmenite, near Mount Painter, Northern Flinders Ranges. *Transactions of the Royal Society of South Australia* 49:101–102.

Brugger, J., Ansermet, S., and Pring, A. (2003) Uranium minerals from Mt Painter, Northern Flinders Ranges, South Australia. *Australian Journal of Mineralogy* 9:15–31.

Brugger, J., Krivovichev, S.V., Berlepsch, P., Meisser, N., Ansermet, S., and Armbruster T. (2004) Spriggite, $Pb_3(UO_2)_6O_8(OH)_2(H_2O)_3$, a new mineral with β-U_3O_8-type sheets: description and crystal structure. *Am Mineral* 89:339–347.

Brugger, J., Long, N., McPhail, D.C., and Plimer, I. (2005) An active amagmatic hydrothermal system: the Paralana Hot Springs, Northern Flinders Ranges, South Australia. *Chem Geol* 222:35–64.

Brugger, J., Meisser, N., Etschmann, B., Ansermet, N. and Pring, A. (2011) Paulscherrerite from the Number 2 Workings, Mt Painter Inlier, Northern Flinders Ranges, South Australia: "dehydrated schoepite" is a mineral after all. *Am Mineral* 96:229–240.

Carlton, A. (2002) A possible sample of the ancient deep hot biosphere from Mt Gee. Unpublished BSc (Hons) thesis, Macquarie University, Sydney, Australia.

Coats, R.P. and Blissett, A.H. (1971) Regional and economic geology of the Mount Painter province. Bulletin 43, Department of Mines, Geological Survey of South Australia, Adelaide.

Dong, G., Morrison, G., and Jaireth, S. (1995) Quartz textures in epithermal veins, Queensland—classification, origin and implication. *Econ Geol* 90:1841–1856.

Drexel, J.F. and Major, R.B. (1987) Geology of the uraniferous breccia near Mt Painter, South Australia and revision of rock nomenclature. *Geological Survey of South Australia Quarterly Notes*, 104, Geological Survey of South Australia, Adelaide.

Druschel, G.K. and Rosenberg, P.E. (2001) Non-magmatic fracture-controlled hydrothermal systems in the Idaho Batholith: South Fork Payette geothermal system. *Chem Geol* 173:271–291.

Elburg, M., Bons, P., Foden, J., and Brugger, J. (2003) A newly defined Late Ordovician magmatic-thermal event in the Mt Painter Province, northern Flinders Ranges, South Australia. *Australian Journal of Earth Sciences* 50:611–631.

Fanning, C.M., Teale, G.S., and Robertson, R.S.I. (2003) Is there a Willyama Supergroup sequence in the Mount Painter Inlier? In *Broken Hill Exploration Initiative,* edited by M. Peljo, Geoscience Australia Record 2003/13, Geoscience Australia, Canberra, pp 38–41.

Fehn, U., Cathles, L.M., and Holland, H.D. (1978) Hydrothermal convection and uranium deposits in abnormally radioactive plutons. *Econ Geol* 73:1556–1566.

Foden, J., Elburg, M.A., Dougherty-Page, J., and Burtt, A. (2006) The timing and duration of the Delamerian Orogeny: correlation with the Ross Orogen and implications for Gondwana assembly. *J Geol* 114:189–210.

Foster, D.A., Murphy, J.M., and Gleadow, J.W. (1994) Middle tertiary hydrothermal activity and uplift of the northern Flinders Ranges, SA: insights from apatite fission track thermochronology. *Australian Journal of Earth Sciences* 41:11–17.

Fournier, R.O. (1985) The behaviour of silica in hydrothermal solutions. In *Geology and Geochemistry of Epithermal Systems,* Reviews in Economic Geology, Vol. 2, edited by B.R. Berger and P.M. Bethke, Society of Economic Geologists, Littleton, CO, pp 45–62.

Grasby, S.E. and Hutcheon, I. (2001) Controls on the distribution of thermal springs in the southern Canadian Cordillera. *Can J Earth Sci* 38:427–440.

Hedenquist, J.W. and Henley, R.W. (1985) Hydrothermal eruptions in the Waiotapu geothermal system, New Zealand: their origin, associated breccias, and relation to precious metal mineralization. *Econ Geol* 80:1640–1668.

Hode, T., Von Dalwigk, I., and Broman, C. (2003) A hydrothermal system associated with Siljan impact structure, Sweden—implications for the search for fossil life on Mars. *Astrobiology* 3:271–289.

Idnurm, M. and Heinrich, C.A. (1993) A palaeomagnetic study of hydrothermal activity and uranium mineralisation at Mt Painter, South Australia. *Australian Journal of Earth Sciences* 40:87–101.

Jackson, S.E., Pearson, N.J., Griffin, W.L., and Belousova, E.A. (2004) The application of laser ablation–inductively coupled plasma–mass spectrometry to *in situ* U-Pb zircon geochronology. *Chem Geol* 211:47–69.

Jagodzinski, E.A. (2005) Compilation of SHRIMP U-Pb geochronological data, Olympic domain, Gawler Craton, South Australia, 2001–2003. *Geoscience Australia Record* G2005/20, Geoscience Australia, Canberra.

Klootwijk, C. (2010) Australia's controversial Middle-Late Palaeozoic pole path and Gondwana-Laurasia interaction. *Palaeoworld* 19:174–185.

Lin, L.H., Wang, P.L., Rumble, D., Lippmann-Pipke, J., Boice, E., Pratt, L.M., Lollar, B.S., Brodie, E.L., Hazen, T.C., Andersen, G.L., DeSantis, T.Z., Moser, D.P., Kershaw, D., and Onstott, T.C. (2006) Long-term sustainability of a high-energy, low-diversity crustal biome. *Science* 314:479–482.

Lindgren, P., Parnell, J., Bowden, S., Taylor, C., Osinski, G.R., and Lee, P. (2009) Preservation of biological markers in clasts within impact melt breccias from the Haughton impact structure, Devon Island. *Astrobiology* 9:391–400.

Lindgren, P., Ivarsson, M., Neubeck, A., Broman, C., Henkel, H., and Holm, N.G. (2010) Putative fossil life in a hydrothermal system of the Dellen impact structure, Sweden. *International Journal of Astrobiology* 9:137–146.

McLaren, S., Dunlap, W.J., Sandiford, M., and McDougall, I. (2002) Thermochronology of high heat-producing crust at Mount Painter, South Australia: implications for tectonic reactivation of continental interiors. *Tectonics* 21:1275–1291.

Mitchell, M.M., Kohn, B.P., O'Sullivan, P.B., Hartley, M.J., and Foster, D.A. (2002) Low-temperature thermochronology of the Mt Painter Province, South Australia. *Australian Journal of Earth Sciences* 49:551–563.

Naumov, M.V. (2002) Impact-generated hydrothermal systems: data from Popigai, Kara, and Puchezh-Katunki impact structures. In *Impacts in Precambrian Shields,* edited by J. Plado and L.J. Peasonens, Springer, Berlin, pp 117–171.

Neumann, N., Sandiford, M., and Foden, J. (2000) Regional geochemistry and continental heat flow: implications for the origin of the South Australian heat flow anomaly. *Earth Planet Sci Lett* 183:107–120.

O'Neill, C., Lenardic, A., Jellinek, A.M., and Kiefer, W.S. (2007) Melt propagation and volcanism in mantle convection simulations, with applications for martian volcanic and atmospheric evolution. *J Geophys Res* 112, doi:10.1029/2006JE002799.

Pace, N.R. (2001) The universal nature of biochemistry. *Proc Natl Acad Sci USA* 98:805–808.

Pidgeon, R.T. (1979) Report on the U-Pb age of monazite samples 930, 931 and 932 (from the Mount Painter area). South Australian Department of Mines and Energy Open File Envelope.

Pirajno, F. and Van Kranendonk, M.J. (2005) Review of hydrothermal processes and systems on Earth and implications for martian analogues. *Australian Journal of Earth Sciences* 52:329–351.

Preston, L.J. and Genge, M.J. (2010) The Rhynie Chert, Scotland, and the search for life on Mars. *Astrobiology* 10:549–560.

Pupin, J-P. (1980) Zircon and granite petrology. *Contrib Mineral Petrol* 73:207–220.

Reid, A.J., Payne, J.L., and Wade, B.P. (2006) A new geochronological capability for South Australia: U-Pb zircon dating via LA-ICPMS. *MESA Journal* 42:27–31.

Sandiford, M. and Quigley, M. (2009) TOPO-OZ: insights into the various modes of intraplate deformation in the Australian continent. *Tectonophysics* 474:405–416.

Sandiford, M., Hand, M., and McLaren, S. (1998) High geothermal gradient metamorphism during thermal subsidence. *Earth Planet Sci Lett* 163:149–165.

Schulte, M., Blake, D., Hoehler, T., and McCollom, T. (2006) Serpentinization and its implications for life on the early Earth and Mars. *Astrobiology* 6:364–376.

Schulze-Makuch, D., Dohm, J.M., Fan, C., Fairen, A.G., Rodriguez, J.A.P., Baker, V.R., and Fink, W. (2007) Exploration of hydrothermal targets on Mars. *Icarus* 189:308–324.

Schwenzer, S.P. and Kring, D.A. (2009) Impact-generated hydrothermal systems capable of forming phyllosilicates on Noachian Mars. *Geology* 37:1091–1094.

Shapiro, R. and Schulze-Makuch, D. (2009) The search for alien life in our Solar System: strategies and priorities. *Astrobiology* 9:335–343.

Shearer, C.K. and Papike, J. (2005) Early crustal building processes on the Moon: models for the petrogenesis of the magnesian suite. *Geochim Cosmochim Acta* 69:3445–3461.

Skok, J.R., Mustard, J.F., Ehlmann, B.L., Milliken, R.E., and Murchie, S.L. (2010) Silica deposits in the Nili Patera caldera on the Syrtis Major volcanic complex on Mars. *Nat Geosci* 3:838–841.

Squyres, S.W., Arvidson, R.E., Ruff, S., Gellert, R., Morris, R.V., Ming, D.W., Crumpler, L., Farmer, J.D., Des Marais, D.J., Yen, A., McLennan, S.M., Calvin, W., Bell, J.F., Clark, B.C., Wang, A., McCoy, T.J., Schmidt, M.E., and de Souza, P.A., Jr. (2008) Detection of silica-rich deposits on Mars. *Science* 320:1063–1067.

Stacey, J.R. and Kramers, J.D. (1975) Approximation of terrestrial lead isotope evolution by a two-stage model. *Earth Planet Sci Lett* 26:207–221.

Teale, G.S. and Flint, R.B. (1993) Curnamona Craton and Mount Painter Province. In *Bulletin 54: The Geology of South Australia,* edited by J.F. Drexel, W.V. Preiss, and A.J. Parker, Mines and Energy Geological Survey of South Australia, South Australia, pp 147–155.

Thomas, M. and Walter, M.R. (2002) Application of hyperspectral infrared analysis of hydrothermal alteration on Earth and Mars. *Astrobiology* 2:335–351.

van Achterbergh, E., Ryan, C.G., and Griffin, W.L. (1999) GLITTER: on-line interactive data reduction for the laser ablation ICP-MS microprobe. In *9th Annual V.M. Goldschmidt Conference*, pp 305–306.

van Middlesworth, P.E. and Wood, S.A. (1998) The aqueous geochemistry of the rare earth elements and yttrium. Part 7. REE, Th and U contents in thermal springs associated with the Idaho Batholith. *Appl Geochem* 13:861–884.

Vance, S., Harnmeijer, J., Kimura, J., Hussmann, H., Demartin, B., and Brown, J.M. (2007) Hydrothermal systems in small ocean planets. *Astrobiology* 7:987–1005.

Veevers, J.J., Belousova, E.A., Saeed, A., Sircombe, K., Cooper, A.F., and Read, S.E. (2006) Pan-Gondwanaland detrital zircons from Australia analysed for Hf-isotopes and trace elements reflect an ice-covered Antarctic provenance of 700–500 Ma age, T-DM of 2.0–1.0 Ga, and alkaline affinity. *Earth Sci Rev* 76:135–174.

Walter, M.R., McLoughlin, S., Drinnan, A.N., and Farmer, J.D. (1998) Palaeontology of Devonian thermal spring deposits, Drummond Basin, Australia. *Alcheringa* 22:285–314.

Willner, A.P., Sindern, S., Metzger, R., Ermolaeva, T., Kramm, U., Puchkov, V., and Kronz, A. (2003) Typology and single grain U/Pb ages of detrital zircons from Proterozoic sandstones in the SW Urals (Russia): early time marks at the eastern margin of Baltica. *Precambrian Res* 124:1–20.

Wülser, P.-A., Meisser, N., Brugger, J., Schenk, K., Ansermet, S., Bonin, M., and Bussy, F. (2005) Cleusonite, $(Pb,Sr)(U^{4+},U^{6+})(Fe^{2+},Zn)_2(Ti,Fe^{2+},Fe^{3+})_{18}(O,OH)_{38}$, a new mineral species of the crichtonite group from the western Swiss Alps. *European Journal of Mineralogy* 17:933–942.

Wülser, P.-A., Brugger, J., Foden, J., and Pfeiffer, H.-R. (2011) The sandstone-hosted Beverley uranium deposit, Lake Frome basin, South Australia: mineralogy, geochemistry and time-constrained model for its genesis. *Econ Geol*, in press.

Yamashita, N., Hasebe, N., Reedy, R.C., Kobayashi, S., Karouji, Y., Hareyama, M., Shibamura, E., Kobayashi, M.N., Okudaira, O., d'Uston, C., Gasnault, O., Forni, O., and Kim, K.J. (2010) Uranium on the Moon: global distribution and U/Th ratio. *Geophys Res Lett* 37, doi:10.1029/2010GL043061.

Address correspondence to:
Joël Brugger
Tectonics, Resources and Exploration
School of Earth and Environmental Sciences
The University of Adelaide
5005 Adelaide
Australia

E-mail: joel.brugger@adelaide.edu.au

Submitted 4 April 2011
Accepted 30 May 2011